International Journal of Coal Science & Technology (2023) 10:55
https://doi.org/10.1007/s40789-023-00609-1

RESEARCH

Revaluating coal permeability-gas pressure relation under various gas pressure differential conditions

Chunguang Wang[1] · Hongxu Wang[1] · Derek Elsworth[2] · Guanglei Cui[3] · Bingqian Li[4] · Meng Zhou[1] · Wenxin Li[1] · Jiyuan Zhang[5]

Received: 4 May 2023 / Revised: 29 May 2023 / Accepted: 18 July 2023

Abstract

Identifying changes in coal permeability with gas pressure and accurately codifying mean effective stresses in laboratory samples are crucial in predicting gas-flow behavior in coal reservoirs. Traditionally, coal permeability to gas is assessed using the steady-state method, where the equivalent gas pressure in the coal is indexed to the average of upstream and downstream pressures of the coal, while ignoring the nonlinear gas pressure gradient along the gas flow path. For the flow of a compressible gas, the traditional method consistently underestimates the length/volume-averaged pressure and overestimates mean effective stress. The higher the pressure differential within the sample, the greater the error between the true mean pressure for a compressible fluid and that assumed as the average between upstream and downstream pressures under typical reservoir conditions. A correction coefficient for the compressible fluid pressure asymptotes to approximately 1.3%, representing that the error in mean pressure and effective stress can be on the order of approximately 30%, particularly for highly pressure-sensitive permeabilities and compressibilities, further amplifying errors in evaluated reservoir properties. We utilized this volume-averaged pressure and effective stress to correct permeability and compressibility data reported in the literature. Both the corrected initial permeability and the corrected pore compressibility were found to be smaller than the uncorrected values, due to the underestimation of the true mean fluid pressure, resulting in an overestimation of reservoir permeability if not corrected. The correction coefficient for the initial permeability ranges from 0.6 to 0.1 (reservoir values are only approximately 40% to 90% of laboratory values), while the correction coefficient for pore compressibility remains at approximately 0.75 (reservoir values are only approximately 25% of laboratory value). Errors between the uncorrected and corrected parameters are quantified under various factors, such as confining pressure, gas sorption, and temperature. By analyzing the evolutions of the initial permeability and pore compressibility, the coupling mechanisms of mechanical compression, adsorption swelling, and thermal expansion on the pore structure of the coal can be interpreted. These findings can provide insights that are useful for assessing the sensitivity of coal permeability to gas pressure as truly representative of reservoir conditions.

Keywords Gas compressibility · Coal permeability · Pressure differential · Mean gas pressure

✉ Chunguang Wang
cgwang@sdust.edu.cn

[1] College of Energy and Mining Engineering, Shandong University of Science and Technology, Qingdao 266590, China

[2] Energy and Mineral Engineering, Geosciences, G3 Center, and EMS Energy Institute, Pennsylvania State University, University Park, PA, USA

[3] Key Laboratory of Ministry of Education On Safe Mining of Deep Metal Mines, Northeastern University, Shenyang 110004, China

[4] Pingdingshan Tianan Coal Mining Co., LTD, Pingdingshan, Henan 467003, China

[5] School of Petroleum Engineering, China University of Petroleum (East China), Qingdao 266580, China

Published online: 26 September 2023

1 Introduction

Assessing controls on coal permeability by effective stresses and gas pressures are important in predicting gas-flow behavior in coal reservoirs (Liu et al. 2020, 2016a, 2015). Current laboratory measurements of rock materials rely on either steady-state or unsteady-state method. The steady-state method measures the rate of fluid flow rate in a rock core under an applied fluid pressure differential, with the permeability evaluated from Darcy's law (Darcy 1856; http.//www.coretest.com/automated-permeameted-porosimeter.html; Liu et al. 2016b; Li et al. 2009). The fluid flow rate may be measured from either the influent rate or effluent rate (Gensterblum et al. 2014a; Cui et al. 2009; Ghanizadeh et al. 2014; Pei et al. 2019), and under steady state, these should be equivalent. Typically, the outlet flow rate is measured. In lowly permeable materials ($< 10^{-18}$ m^2) flow rates are difficult to measure using flow-meters and steady conditions must take an extended period to stabilize Thus, pulse decay metods (Brace et al. 1968) utilize the unsteady response where a transient pressure differential is applied at the two ends of a pre-saturated rock core. The resulting permeability is evaluated from the pressure equilibration rate between the upstream and downstream reservoirs or the time to reach equilibrium.

Different from single porosity media, fractured coals contain complex cleat networks and micro-pores in matrix blocks with significantly different porosities and permeabilities (Laubach et al. 1998; Chen et al. 2015; Connell et al. 2016; Gensterblum et al. 2015, 2014b). The maximum permeability is typically in the high porosity fractures and cleats and is strongly influenced by changes in cleat aperture (Levine 1996; Palmer and Mansoori 1998; Wang et al. 2022; Wang et al. 2021a; Shi and Durucan 2004a; Liu and Rutqvist 2010; Pan and Connell 2011; Liu et al. 2011).Since permeability is strongly effective-stress- or pressure-dependent, two end-member deformability boundary conditions are typically applied (Harpalani and Chen 1997; Chen et al. 2011; Meng and Li 2017; Seomoon et al. 2015). One boundary condition is to control bulk deformation as either uniaxial deformation (Geertsma 1966) or fully constrained deformation. The other boundary condition is to control the tri-axial stress state as either a constant confining-pressure or constant effective-stress. Numerous experimental results have demonstrated that if the flow regime of the percolating fluid remains viscous, then coal permeability is positively related to gas pressure (Pini et al. 2009; Harpalani and Schraufnagel 1990; Wang et al. 2011; Kumar et al. 2015). If the gas flow regime shifts from slippage flow to viscous flow due to increasing gas pressure, the resultant coal permeability to first decrease and then partially rebound (Wang et al. 2019). When the effective stress remains unchanged, the coal permeability varies negatively with increasing pore pressure.

Numerous theoretical models have been developed to interpret the impacts of mechanical compression and adsorption-induced swelling on coal permeability (Gray 1987; Seidle and Huitt 1995; Palmer and Mansoori 1996; Palmer et al. 2007; Shi and Durucan 2004b, 2005; Cui and Bustin 2005). The pore deformability of coal are significantly impacted by coal compressibility. Since coal reservoirs exist in particular regimes of temperature, moisture, fluid properties, and geo-stress, the coal compressibility coefficient must be quantitatively assessed as influenced by these parameters (Robertson and Christiansen 2005; Shi and Durucan 2004c, 2010; McKee et al. 1988; Palmer 2009; Pan et al. 2010; Harpalani 1999). For example, the water-based or helium-based compressibility coefficient of coal is a positive constant, if the effective stress varies only over a small range. In contrast, the pore compressibility coefficient varies with changes in the pore pressure when the effective stress varies over a wider range. More importantly, gas-adsorption-induced swelling effects further complicate the change in porosity of the coal, whereby the compressibility coefficient may be negative (Liu and Harpalani 2014; Harpalani and Mitra 2010). Therefore, accurate characterization and measurement of the coal permeability-gas pressure relation is a prerequisite for investigating the poromechanical response of coal reservoirs.

In the most frequently used steady-state method, the fluid-pressure-gradient term of Darcy's formula may be modified by the impact of fluid compressibility (Chen 1994). For steady flow with an incompressible fluid (i.e. water), coal permeability k is calculated as:

$$k = -\frac{Q\mu L}{A(P_{\mathrm{down}} - P_{\mathrm{up}})} \tag{1}$$

where Q is gas flow rate, μ is gas viscosity, L is flow length within the medium, x is seepage distance and P_{down} and P_{up} denote the downstream and upstream pressures, respectively. The pressure distribution of the incompressible fluid along the flow distance x is

$$p = \frac{P_{\mathrm{down}} - P_{\mathrm{up}}}{L}x + P_{\mathrm{up}} \tag{2}$$

For a compressible fluid, the coal permeability in the steady state is determined from:

$$k = \frac{-2Q\mu LP_{\mathrm{down}}}{A\left(P_{\mathrm{down}}^2 - P_{\mathrm{up}}^2\right)} \tag{3}$$

and the nonlinear pressure distribution along the flow distance x (Dana and Skoczylas 1999):

$$p = \sqrt{P_{\text{up}}^2\left(1 - \frac{x}{L}\right) + P_{\text{down}}^2 \frac{x}{L}} \tag{4}$$

Figure 1 compares the two pressure distributions of incompressible and compressible fluids for identical upstream and downstream pressures, identifying linear and nonlinear distributions. Importantly, for a compressible fluid both the central and length/volume-weighted mean pressures are greater than the average of the upstream and downstream pressures. Thus, care must be taken in referencing the measured permeability magnitudes to a pressure or effective stress representative of the experiment – that is not always the average of upstream and downstream bounding magnitudes.

In the following we quantify the representative length/volume-weighted mean pressure of the fluid under a prescribed pressure differential across a porous medium. The corrected mean pressure is always greater than the uncorrected mean pressure. We use this reevaluation to correct published magnitudes for coal permeability as a function of gas pressure and define the magnitude of the overestimation, if the mean of upstream and downstream pressures is merely used as the reference pressure. Pore compressibility coefficients from the literature are similarly corrected in the present work, and their variations with confining pressure, gas sorption, and temperature are discussed. The use of a corrected pressure method is shown capable of defining a more precise relationship between coal permeability and gas pressure, especially where significant pressure differentials are applied in experiments.

2 Mean pressure of gas along one-dimensional flow path

The mean pressure of gas along one-dimensional flow path may be determined from the integral of the pressure distributions shown in Fig. 1. For an incompressible fluid (Eq. (2)),

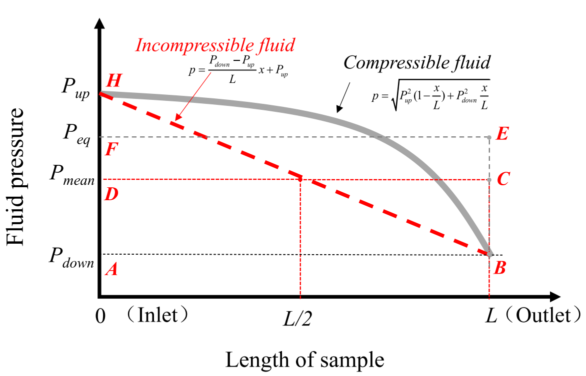

Fig. 1 Schematic of fluid-pressure-distribution along a flow path for compressible and incompressible fluids

the integral domain (ABH) is the equivalent of a uniform distribution given by the rectangle (ABCD). The mean pressure p_{mean} is the height of this rectangle (0D), as:

$$p_{\text{mean}} = \frac{\int_0^L \left(\frac{P_{\text{down}} - P_{\text{up}}}{L}x + P_{\text{up}}\right)\text{d}x}{L} = \frac{P_{\text{up}} + P_{\text{down}}}{2} \tag{5}$$

Clearly, this result demonstrates that the mean pressure of an incompressible fluid is the average of the upstream and downstream pressures. Similarly, the mean pressure of a compressible fluid p_{eq} is the height of the rectangle, as:

$$p_{\text{eq}} = \frac{\int_0^L \sqrt{p_{\text{up}}^2\left(1 - \frac{x}{L}\right) + p_{\text{down}}^2 \frac{x}{L}}\text{d}x}{L} = \frac{2}{3}\frac{p_{\text{up}}^2 + p_{\text{up}}p_{\text{down}} + p_{\text{down}}^2}{p_{\text{up}} + p_{\text{down}}} \tag{6}$$

Figure 2a compares the mean pressure values of compressible fluid and incompressible fluid under various combinations of upstream and downstream pressures. It is clearly seen that when the downstream pressure is 0.1 MPa (atmospheric pressure), the larger the upstream pressure is, the higher the mean pressure of compressible fluid is than the incompressible fluid pressure. If the downstream pressure is 3.0 MPa, the mean pressure of a compressible fluid is approximately equal to that of an incompressible fluid.

In order to correct for this error in evaluating mean fluid-pressure for the effect of fluid compressibility, a correction coefficient $p_{\text{eq}} = \lambda p_{\text{mean}}$ is defined as the ratio of the compressible fluid pressure $p_{\text{eq}} = \lambda p_{\text{mean}}$ to the incompressible fluid pressure $p_{\text{eq}} = \lambda p_{\text{mean}}$, as expressed by:

$$p_{\text{eq}} = \lambda p_{\text{mean}} \tag{7}$$

Figure 2b displays this relationship between the correction coefficient of gas pressure $k_\infty^{\text{eq}} = \lambda_k k_\infty$ and the upstream pressure for a certain downstream pressure. The higher the downstream pressure, the closer $k_\infty^{\text{eq}} = \lambda_k k_\infty$ is to unity. It should be noted that for the steady-state method of permeability measurement, the downstream pressure of coal sample is typically set to atmospheric, which would be 0.1 MPa (absolute) in this case. Thus, $k_\infty^{\text{eq}} = \lambda_k k_\infty$ is approximately 1.3, if the upstream pressure > 3 MPa.

3 Permeability observations corrected for gas pressure

It is apparent from Fig. 2a and b that a lower pressure differential can approximately linearize distribution curve of gas pressure. In this paper, therefore, the presented method (Eq. (6)) is used to evaluate coal permeability for larger pressure differential case, in which case gas slip occurring in lower gas pressure is ignored. We use the McKee et al.

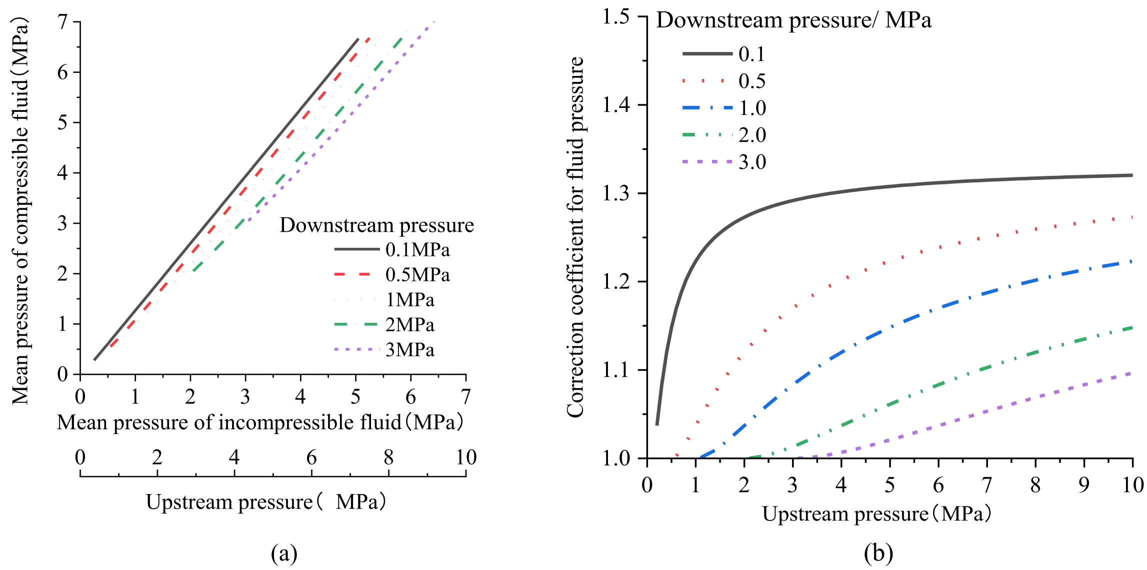

Fig. 2 Relationship between mean incompressible and compressible fluid pressures with varying upstream and downstream pressures. **a** Mean pressure of incompressible and compressible fluids; **b** Change in correction-coefficient

Table 1 Compilation of published experimental data

References	Confining pressure (MPa)/ Temperature (°C)	Gas type	Length of coal sample (mm)	Upstream pressure (MPa)	Downstream pressure (MPa)
Han et al. (2010)	10, 15, 20, 30, 40/-	Ar	21.2 22.5	0.3–8	0.1
Meng et al. (2015)	3.5/11.5	He, N_2, CO_2	100	< 2.5	0.1
Wang et al. (2017)	4, 8/40	CO_2, CH_4, He	100	0.5,1,1.5,2,3	0.1
Dai (2020)	2, 4, 6, 8, 10/-	CH_4	100	1–6	0.1
Gao et al. (2021)	6/30, 40, 50, 60	CH_4	100	0.2–1.8	0.1
Teng et al. (2021)	6,10,15,20 / 25, 45, 65, 90	CO_2	80–100	1,2,3,4,5,6	0.1
Yanguang (2019)	1,2,3,4,5/-	CH_4	100	0.6–1.4	0.1
Feng (2021)	1.5, 2.3, 3.9, 4.7/30	CH_4, CO_2		0.2–1 0.3–1.5	0.1

(1988) permeability model to fit several groups of the laboratory dataset using the published literature. The relation is:

$$k = k_\infty \cdot e^{-3C_f(\sigma_c - p)} \tag{8}$$

where $k_\infty^{eq} = \lambda_k k_\infty$ is the initial permeability of coal. $k_\infty^{eq} = \lambda_k k_\infty$ is a measure of unjacketed permeability that is subjected to hydrostatic pressure—equivalent to the pore pressure p being equal to the confining pressure $k_\infty^{eq} = \lambda_k k_\infty$. $k_\infty^{eq} = \lambda_k k_\infty$ is the pore compressibility coefficient. Two correction coefficients for the initial permeability and the pore compressibility are defined as the ratio of the corrected value and the uncorrected value, respectively: $k_\infty^{eq} = \lambda_k k_\infty$ for the initial permeability (Eq. (9)) and $k_\infty^{eq} = \lambda_k k_\infty$ for the pore compressibility (Eq. (10)):

$$k_\infty^{eq} = \lambda_k k_\infty \tag{9}$$

$$C_f^{eq} = \lambda_c C_f \tag{10}$$

3.1 Impacts of confining pressure

We use three groups of published data correcting the permeability—pore pressure relation to evaluate the impacts of confining pressure. These are for non-sorbing Ar permeability at confining pressures of 10–30 MPa (Han et al. 2010) and for sorbing CH_4 permeability at 4–7 MPa (Dai 2020) and CH_4 permeability at 6–15 MPa (Teng et al. 2021), as listed in Table 1. These are corrected using Eq. (4). From

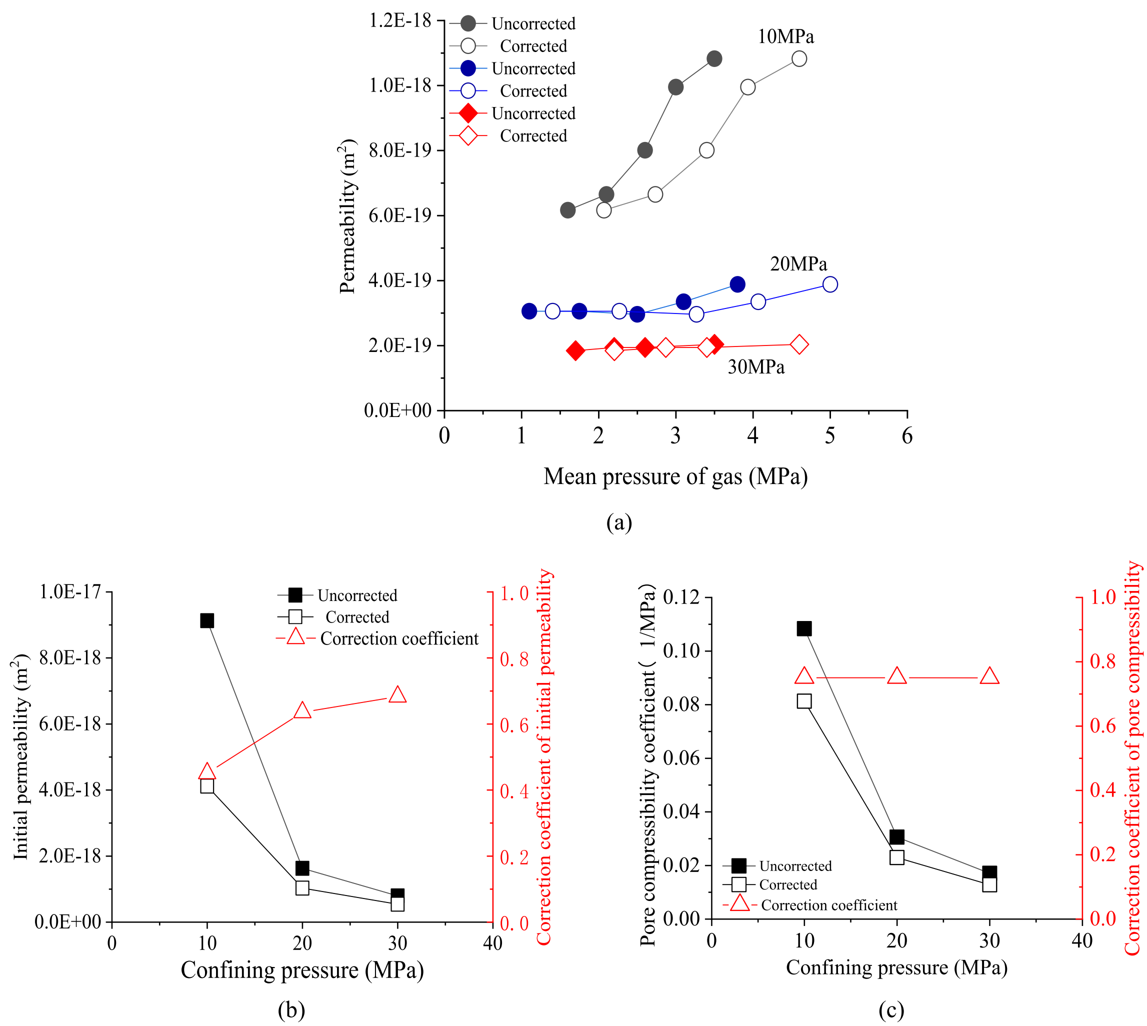

Fig. 3 Relationship between coal permeability and Ar pressure for different confining pressures (Han et al. 2010). **a** Coal permeability corrected for Ar pressure; **b** Fitted initial permeabilities corrected for Ar pressure; **c** Pore compressibilityies corrected for Ar pressures

Figs. 3a, 4a, and 5a, it is clear that all of the permeability-corrected pore-pressure curves move to elevated pore-pressures indicating that coal-permeabilities are always overestimated if the uncorrected pressures are used.

Using Eq. (8), both the initial permeability and the pore compressibility of the coals are fitted by the corrected and uncorrected gas-pressure relationships, respectively. The fitting parameters are plotted in Figs. 3b and c. Both the initial permeability and the pore compressibility of the coal decrease as the confining pressure rising, identifying that the coal matrix skeleton contracts under the pore pressure, in which case the pore pressure is equal to the external stress (or confining pressure). Nevertheless, the two parameters that are fitted by the corrected gas pressure are less than those that are fitted by the uncorrected gas pressure. Consequently, the correction coefficient of the initial permeability increases from 0.4 to 0.7, while the correction coefficient of the pore compressibility remains at approximately 0.75.

3.2 Impacts of gas sorption

Gas-sorption effects can significantly change the evolution of coal permeability with gas pressure. CO_2 exhibits a stronger affinity for coal than does CH_4, while the adsorption of N_2 is the weakest. The larger the gas-sorption capacity is, the greater the decreasing amplitude of coal permeability becomes (Meng et al. 2015; Wang et al. 2017, 2021b; Feng 2021). The pressure-corrected relationships between permeability and gas pressure from this dataset are shown in Figs. 6a, b, and c. Since the mean pressure of the gas will be underestimated for a compressible gas, the corresponding coal permeability will be overestimated. Figure 7a compares the corrected initial permeability with the uncorrected permeability. For the cases using He, N_2, CO_2, and CH_4, the corrected initial permeability is found to be generally lower than the uncorrected one. The relationship between the magnitude of the initial permeability and the

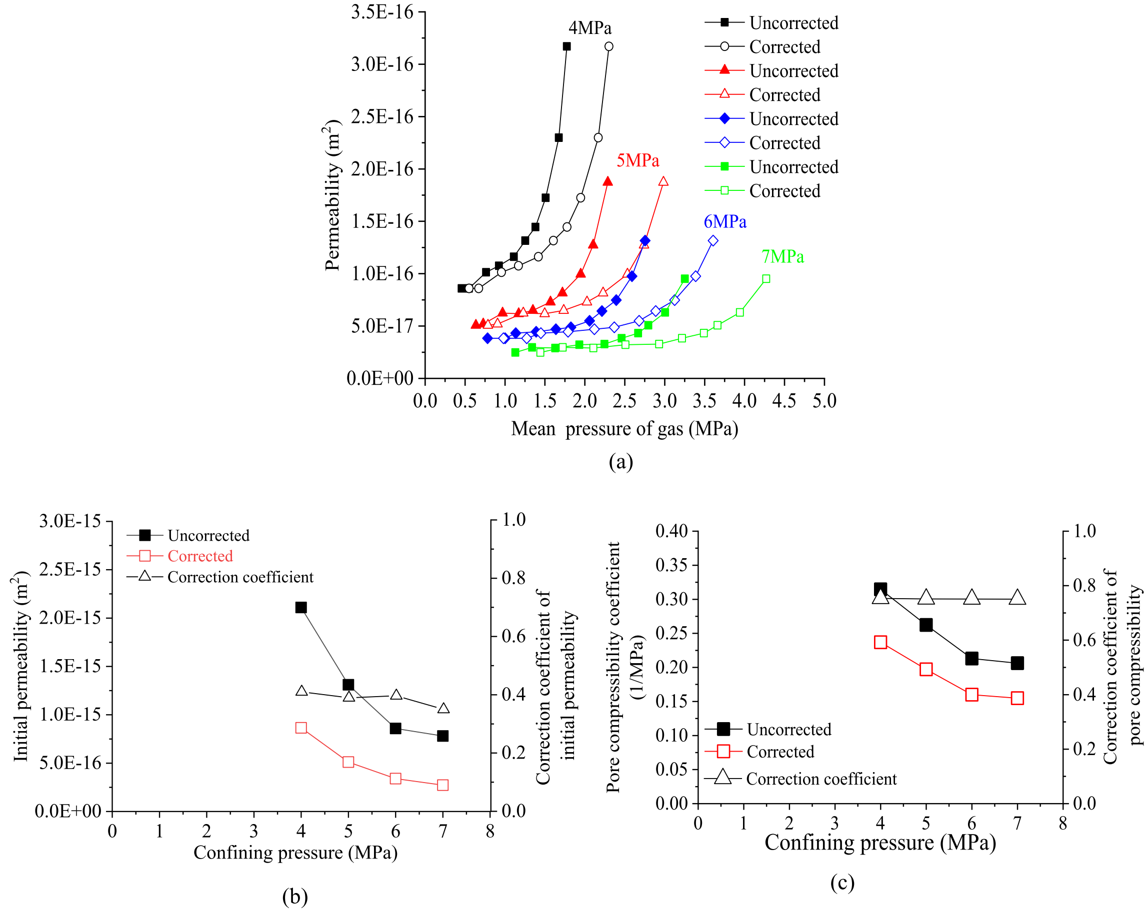

Fig. 4 Coal permeability—CH_4 pressure curves under different confining pressures (Dai 2020). **a** Coal permeability corrected for CH_4 pressure; **b** Initial permeability corrected for CH_4 pressure; **c** Pore compressibility corrected for CH_4 pressure

gas absorbability is not clear, which is likely due both to the heterogeneity of different coals and to the applied stress states. Nevertheless, the correction coefficient for the initial permeability remains in the range between 0.6 and 0.8, as shown in Fig. 7b. Similarly, the corrected pore compressibility is also lower than the uncorrected compressibility, as shown in Fig. 8a. Although the pore compressibility of different coals is related to the gas species, the relevant correction coefficients are approximately 0.75 (Fig. 8b).

3.3 Impacts of thermally-induced expansion

The heating of coal typically results in an inhomogeneous expansion and the cracking between minerals, organic matter, and inorganic matter (Heuze 1983; Wong and Brace 1979) as well as to gas desorption (Charrière et al. 2010; Deishad et al. 2009) with these multi-physical processes potentially affecting permeability. From the literature (Gao et al. 2021; Teng et al. 2021), coal permeability can clearly be seen to decrease with increasing ambient temperature. By correcting the experimental dataset, Figs. 9a and 10a indicate that all of the coal-permeability-corrected gas-pressure curves translate to higher equivalent pore-pressures. Thus, if the pressures remain uncorrected then the corresponding coal permeability will be overestimated. As shown in Figs. 9b and 10b, both the corrected initial permeability and the corrected pore compressibility are lower than the uncorrected magnitudes. The correction coefficients of the initial permeability and the pore compressibility are approximately 0.5 for Fig. 9c and 0.75 for Fig. 10c, respectively.

4 Discussion

4.1 Error analysis of the permeability-to-mean-gas-pressure relation

The aforementioned data of Figs. 3, 4, and 5 demonstrate that coal permeability will rise exponentially with increasing gas pressure, if the confining pressure remain unchanged at a certain isothermal condition. As shown in Fig. 11a, because

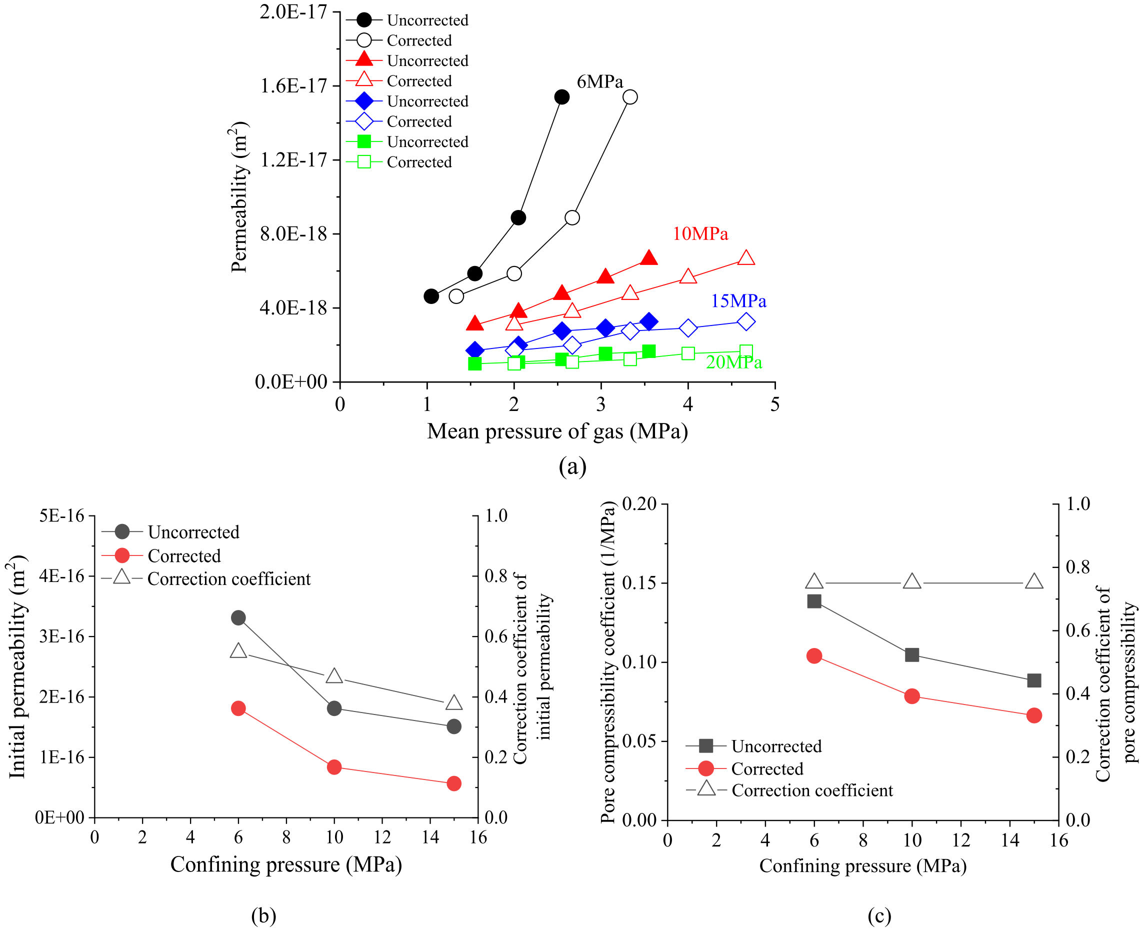

Fig. 5 CH_4 pressure-dependent coal permeability under different confining pressures (Teng et al. 2021). **a** Coal permeability corrected for CH_4 pressure; **b** Initial permeability corrected for CH_4 pressure; **c** Pore compressibility corrected for CH_4 pressure

the corrected permeability curves translate rightward to higher pressures, the absolute error between the corrected permeability and the uncorrected permeability increases correspondingly.

Based on the literature data (Dai 2020), Fig. 11b compares the relative error between the corrected permeability and the uncorrected permeability under four confining-pressure conditions ranging from 4 to 7 MPa. For any of four confining pressure condition, the rising pore pressure can cause the relative error to first increases and then decrease. At the case of a confining pressure of 4 MPa, when the pore pressure ranges below 1.5 MPa, the error is within 10%, but when the pore pressure increases to 2.5 MPa, the error peaks at 200%.

Under various isothermal conditions from Figs. 9a and 10a, it is reasonably assumed that coal permeability can be defined as a logarithmic function of gas pressure, whereby the incremental permeability decreases with the gas pressure rising. As a result, Fig. 12a demonstrates that the absolute error between the corrected permeability and the uncorrected permeability also decreases with the gas pressure rising. Changes in the corresponding relative error under four different temperatures are shown in Fig. 12b. As can be seen, the relative error first increases and then peaks from between 10% at 0.5 MPa under 20 °C and 15% at 0.7 MPa under 40 °C. It is found that the higher the isothermal condition is, the greater the relative error becomes.

4.2 Implications for pore deformation due to coal–gas interaction

It is well known that the effective stress is defined by the portion of the external stress which is supported by the solid skeleton of the porous medium, while the remaining external stress carried by the pore fluid. Any change in effective stress reduces the pore radius and hence the permeability of a single pore in an impermeable medium. Unlike the single-pore medium, the matrix blocks in coal are permeable and can usually be simplified as an assemblage of discrete grains that contain connected and closed micropores. When gas

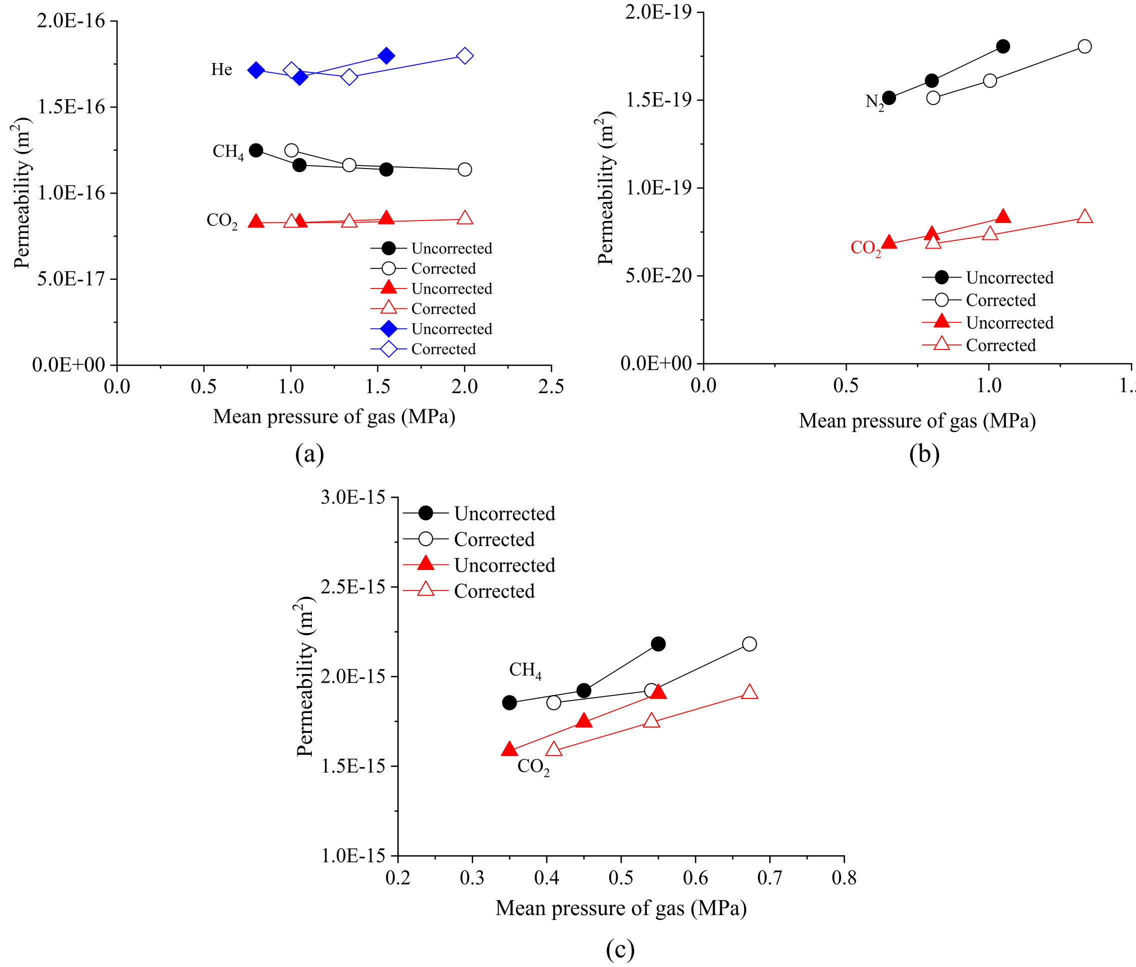

Fig. 6 Coal-permeability versus pressure relationships for injection of different gases. **a** From reference (Wang et al. 2017); **b** From reference (Meng et al. 2015); **c** From reference (Feng 2021)

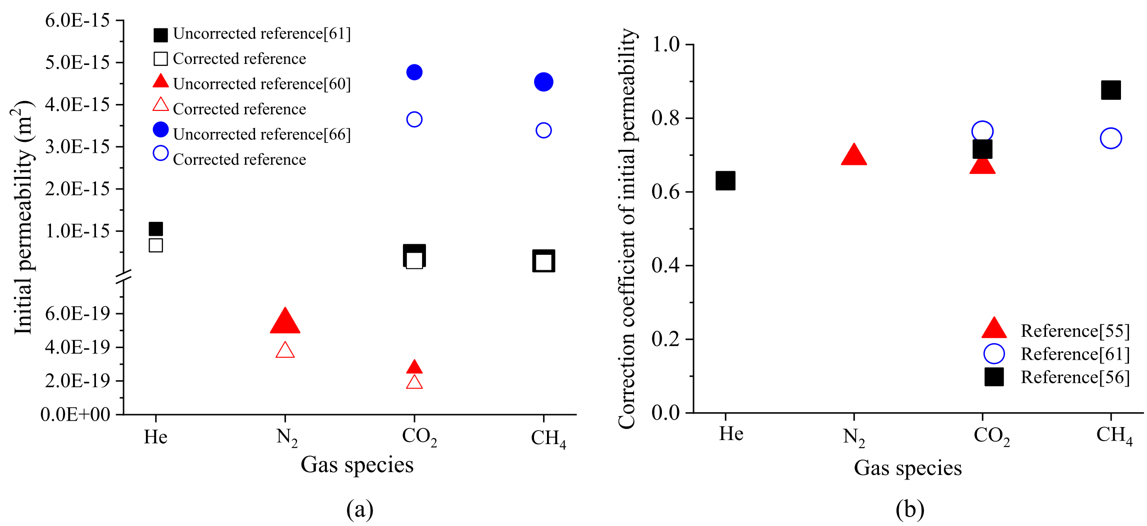

Fig. 7 Comparison between uncorrected initial permeability and corrected permeability for different gases. **a** Corrected initial permeability; **b** Correction coefficient for initial permeability

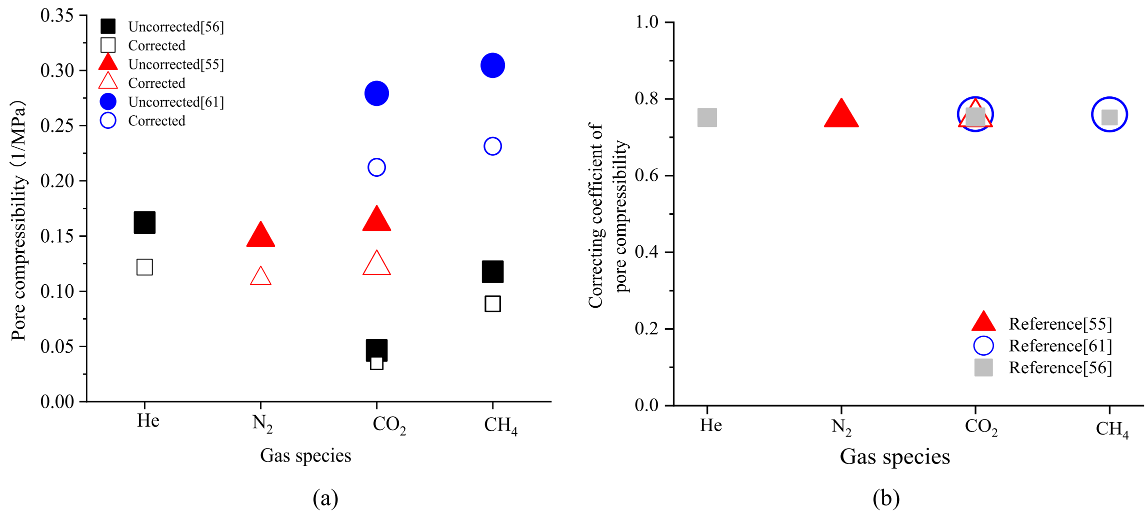

Fig. 8 Comparison between uncorrected pore compressibility and corrected compressibility for different gases. **a** Corrected pore compressibility; **b** Correction coefficient for pore compressibility

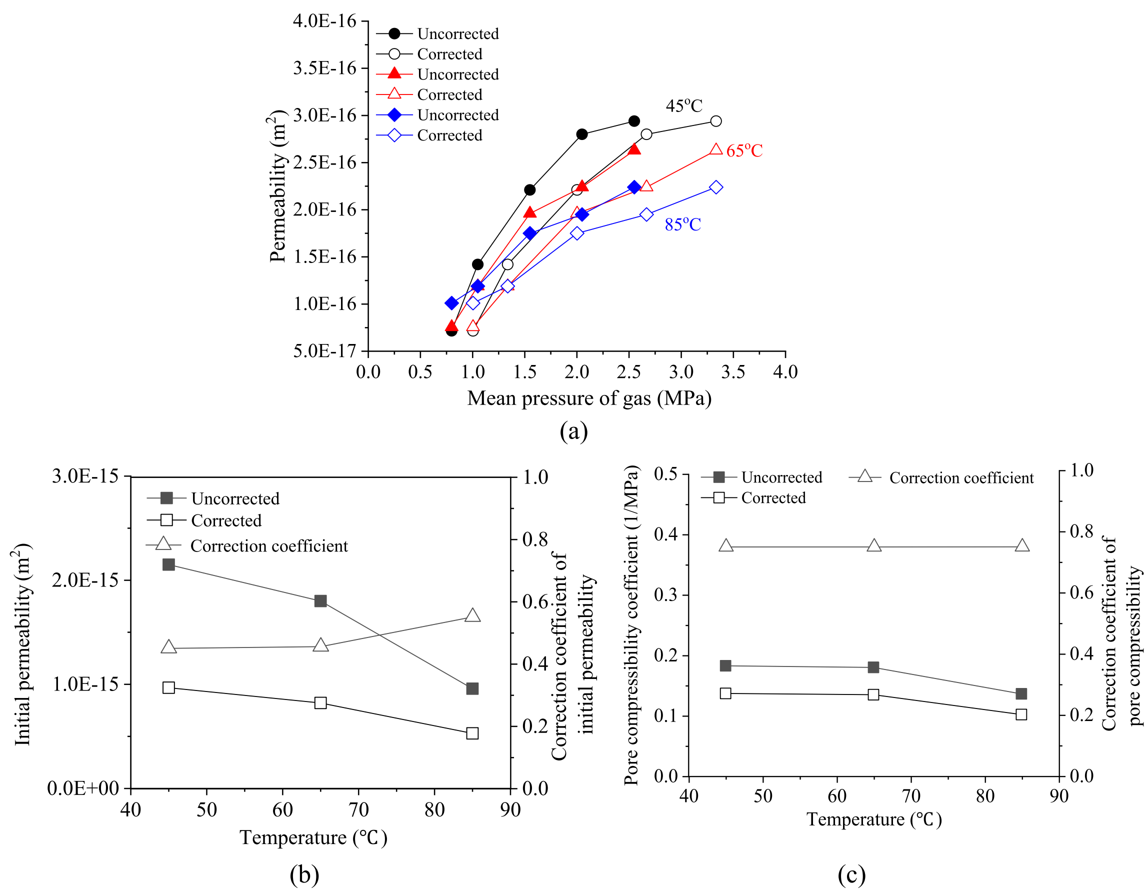

Fig. 9 Correlations of coal permeability with CH_4 pressure for variable temperatures (Teng et al. 2021). **a** Coal permeability corrected for CH_4 pressure; **b** Fitted initial permeability for corrected CH_4 pressure; **c** Fitted pore compressibility for corrected CH_4 pressure

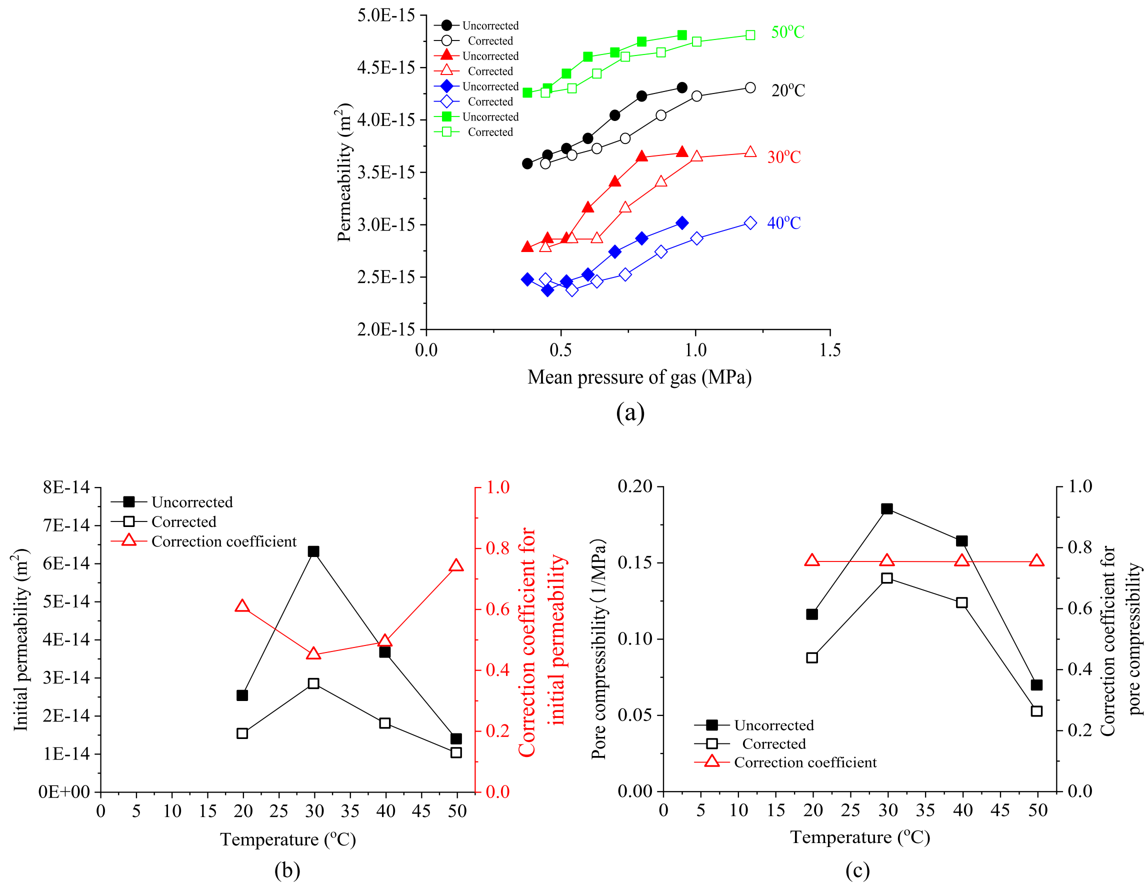

Fig. 10 Correlations of coal permeability with CH_4 pressure for variable temperatures (Gao et al. 2021). **a** Coal permeability corrected for CH_4 pressure; **b** Fitted initial permeability for corrected CH_4 pressure; **c** Fitted pore compressibility for corrected CH_4 pressure

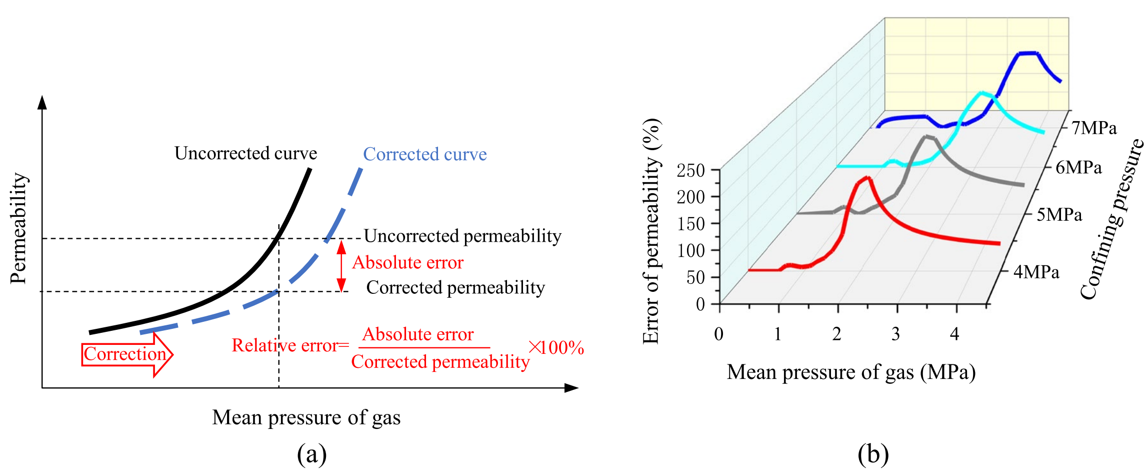

Fig. 11 Error analysis for the relationship between coal permeability and corrected gas pressure under different confining pressure conditions (Dai 2020). **a** Relative error calculation for permeability; **b** Relative error of permeability with gas pressure and confining pressure

flows into the coal, the gas pressure resists not only a part of the external stress, but also the internal stresses among the grains in the matrix. Fjaer et.al. (2008) argue that as the pore pressure rises, a greater proportion of the external stress is counteracted by the pore pressure. The remaining external stress that acts on the matrix accordingly decreases, which can cause the grains in the matrix to expand. This argument can be demonstrated by the observed decrease in

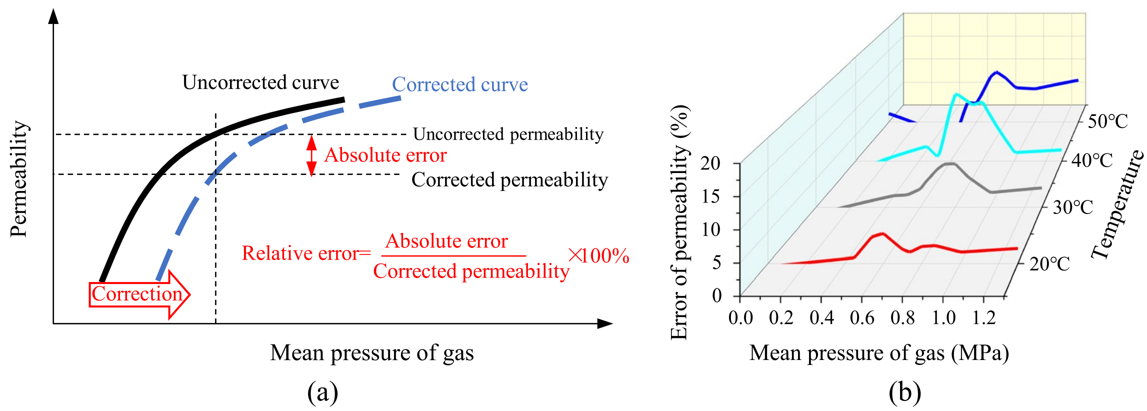

Fig. 12 Error analysis for the relationship between coal permeability and corrected gas pressure under different isothermal conditions (Gao et al. 2021). **a** Relative error calculation for permeability; **b** Relative error of permeability with gas pressure and temperature

coal permeability with increasing pore pressure under the constant effective stress (Seomoon et al. 2015). In fact, the stress state of the presented initial permeability is an extreme condition in the constant-effective-stress case—namely zero effective stress. In this case, Han's (2010) work demonstrated that the initial permeability of coal to Ar decreases with increasing confining pressure, which is consistent with laboratory observations under non-zero effective-stress cases. This finding indicates that coal-matrix swelling not only enlarges the overall size of the coal, but also consequently reduces the fracture (or void) volume. This interplay between coal matrix and facture is shown schematically in Fig. 13. In addition to the mechanical compression shown here, gas adsorption may also cause the coal matrix to swell, whereby a part of the matrix-swelling strain can also reduce the void volume and narrow fractures, as was demonstrated in Wang's observations (Wang et al. 2021b).

Given that molecular motion in gases is sensitive to temperature, the thermal impacts of gas-bearing coal on permeability are significantly controlled via competition between the gas-desorption-induced shrinkage of the matrix and the thermal expansion of the matrix. Figure 10b reveals that the initial permeability of the coal first increases and then decreases if temperatures are raised from 20 to 50 °C. We postulate that the permeability enhancement at lower temperature is dominated by the impacts of gas-desorption-induced shrinkage of the matrix, while the subsequent reduction might result from the thermal expansion of the matrix at higher temperature. In contrast, Teng's (Teng et al. 2021) observations suggest that the initial permeability of

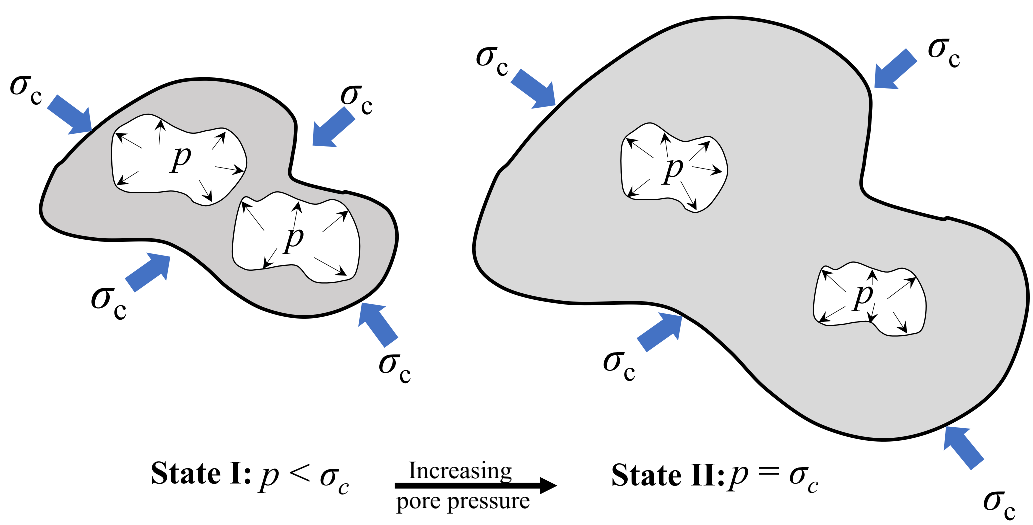

Fig. 13 Schematic diagram of pore (white) deformation induced by expansion of the coal matrix (blue). State I denotes an initial stage, in which case the confining pressure σ_c is higher than the pore pressure p. State II denotes an equilibrium state, in which the pore pressure p is increased to the confining pressure σ_c. As a result, the pore volume is reduced due to expansion of the coal volume

coal declines with temperature rising from 45 to 85 °C. It seems probable that the thermal expansion of the matrix (linear with temperature and unbounded) could exceed the desorption-induced shrinkage of the matrices (nonlinear and bounded by a finite mass of desorbing gas), in which case, a portion of the expanding matrix could decrease the fracture volume.

5 Conclusions

We identify the need to define effectives stresses in samples via a volume-averaged pore pressure representative of the flow path. This is necessary to correctly index the effective-stress-dependent and pressure-dependent nature of permeability, pore compressibility and sorption to the correct reference stresses and allow laboratory observations to be matched to reservoir data. We develop a straightforward method to calculate the mean (volume-averaged) pressure of compressible fluids transiting a porous medium. We apply this method to existing data representative of laboratory observations of permeability, pore compressibility and sorption conducted at equivalent reservoir conditions and show that reference pressures may be in error by 0% to approximately 30%. Since permeability is a sensitive and nonlinear function of effective stress, permeabilities may be overestimated by 40%–90% and pore compressibilities by approximately 25%—thus the effect is significant. We draw the following conclusions:

(1) The higher the pressure differential between the two ends of a porous medium, the greater the mean pressure of the compressible fluid relative to the average for an incompressible fluid. A correction coefficient for the mean pressure for the compressible fluid pressure is defined relative to the assumed mean pressure of the incompressible fluid (i.e. the average of upstream and downstream pressures). Where the effluent/downstream pressure is atmospheric the correction coefficient asymptotes to approximately 1.3 for reasonable reservoir conditions and gases (i.e. upstream pressure > 3 MPa)—defining a 30% error.

(2) Laboratory measured permeabilities and pore compressibilities present in the literature data were corrected with the method. If the mean pressure of the gas under a certain pressure differential is not corrected for compressibility, then the laboratory-interpreted permeability will overestimate the real permeability in the reservoir. If the confining pressure remain unchanged, the absolute error between the corrected permeability and the uncorrected permeability begin to accumulate, as the pore pressure increases; the relative error of the permeability under a certain confining pressure first increases and then decreases. As the isothermal level is elevated, the incremental permeability decreases with the gas pressure rising. The absolute error between the corrected permeability and the uncorrected permeability also decreases with increasing gas pressure. The relative error first increases with increasing gas pressure and then peaks from between 10% at 0.5 MPa under 20 °C and 15% at 0.7 MPa under 40 °C. The higher the coal temperature is, the greater the relative error becomes.

(3) Poroelastic parameters of the McKee (McKee et al. 1988) model are fitted from both the corrected and uncorrected datasets. Both the corrected initial permeability and the corrected pore compressibility were found to be smaller than the uncorrected magnitudes, due to the underestimation of true mean fluid pressure. The correction coefficient for the initial permeability ranges widely but in the range approximately 0.6 to 0.1 (approximately 40% to 90%), while the correction coefficient for pore compressibility remains at approximately 0.75 (approximately 25%).

(4) According to the fitted the initial permeability and the pore compressibility of coal under different conditions, such as, confining pressure, gas adsorption and temperature, it is reasonably demonstrated that the swelling or expansion of the coal matrix block can not only increase the overall size of the coal, but also reduce the coal fracture aperture to a certain extent. This finding can provide a critical insight into evaluating the poroelastic behavior of a coal.

Acknowledgements The present work was made possible with the financial support of the National Natural Science Foundation of China (12002081 42102338, 42202323) and the Natural Science Foundation of Shandong Province (ZR2019MA009). The Technology Improvement Project of Small and Medium Enterprise in Shandong Province, China (2021TSGC1100), is also gratefully acknowledged. Derek Elsworth acknowledges support from the G. Albert Shoemaker endowment.

Declarations

Competing interests The authors have no competing interests to declare that are relevant to the content of this article.

References

Brace W, Walsh JB, Frangos WT (1968) Permeability of granite under high pressure. J Geophys Res B 73(6):2225–2236

Charrière D, Pokryszka Z, Behra P (2010) Effect of pressure and temperature on diffusion of CO2 and CH4 into coal from the Lorraine basin (France). Int J Coal Geol 81:373–380

Chen G (1994) Gas slippage and Matrix Shrinkage Effects on Permeability of Coal. The University of Arizona, USA. PhD thesis.

Chen Z, Pan Z, Liu J, Connell LD, Elsworth D (2011) Effect of the effective stress coefficient and sorption-induced strain on the evolution of coal permeability: experimental observations. Int J Greenh Gas Control 5(5):1284–1293

Chen T, Feng XT, Pan Z (2015) Experimental study of swelling of organic rich shale in methane. Int J Coal Geol 150:64–73

Connell LD, Mazumder S, Sander R et al (2016) Laboratory characterization of coal matrix shrinkage, cleat compressibility and the geomechanical properties determining reservoir permeability. Fuel 165:499–512

Cui X, Bustin RM (2005) Volumetric strain associated with methane desorption and its impact on coalbed gas production from deep coal seams. AAPG Bull 89(9):1181–1202

Cui X, Bustin AMM, Bustin RM (2009) Measurements of gas permeability and diffusivity of tight reservoir rocks, different approaches and their applications. Geofluids 9:208–223

Dai J (2020) Experimental study on the influence of multiple factors on coal permeability technology 39(6): 4

Dana E, Skoczylas F (1999) Gas relative permeability and pore structure of sandstones. Int J Rock Mech Min Sci 36(5):613–625

Darcy H (1856) Les fontaines publiques de la ville de Dijon. Dalmont, Paris

Deishad M, Thomas SG, Wheeler MF (2009) Parallel numerical reservoir simulations of non-isothermal compositional flow and chemistry. In: SPE Reservoir Simulation Symposium Proceedings The Woodlands, TX

Feng Z (2021), Experimental research on CO_2 enhanced coalbed methane recovery. Chongqing University, China, Master thesis

Fjaer E, Holt RM, Horsrud P, Raaen AM (2008) Petroleum related rock mechanics. Elsevier, Amsterdam

Gao Z, Li B, Li J et al (2021) Coal permeability related to matrix-fracture interaction at different temperatures and stresses. J Petrol Sci Eng 200:108428

Geertsma J (1966) Problems of rock mechanics in petroleum production engineering. In: 1st ISRM Congress 3, pp 585–594

Gensterblum Y, Ghanizadeh A, Krooss BM (2014a) Gas permeability measurements on Australian subbituminous coals, fluid dynamic and poroelastic aspects. J Nat Gas Sci Eng 19:202–214

Gensterblum Y, Ghanizadeh A, Krooss BM (2014b) Gas permeability measurements on Australian subbituminous coals: fluid dynamic and poroelastic aspects. J Nat Gas Sci Eng 19:202–214

Gensterblum Y, Ghanizadeh A, Cuss RJ et al (2015) Gas transport and storage capacity in shale gas reservoirs—a review. Part A, transport processes. J Unconv Oil Gas Resour 12:87–122

Ghanizadeh A, Gasparik M, Amann-Hildenbrand A et al (2014) Experimental study of fluid transport processes in the matrix system of the European organic-rich shales I. Scandinavian Alum Shale. Mar Pet Geol 51:79–99

Gray I (1987) Reservoir engineering in coal seams: part 1—the physical process of gas storage and movement in coal seams. SPE Reserv Eng 2(1):28–34

Han F, Busch A, Krooss BM et al (2010) Experimental study on fluid transport processes in the cleat and matrix systems of coal. Energy Fuels 24(12):6653–6661

Harpalani S (1999) Compressibility of coal and its impact on gas production from coalbed reservoirs. In: Vail Rocks 1999, The 37th US Symposium on Rock Mechanics (USRMS). OnePetro.

Harpalani S, Chen G (1997) Influence of gas production induced volumetric strain on permeability of coal. Geotech Geol Eng 15(4):303–325

Harpalani S, Mitra A (2010) Impact of CO_2 injection on flow behavior of coalbed methane reservoirs. Transp Porous Media 82(1):141–156

Harpalani S, Schraufnagel RA (1990) Shrinkage of coal matrix with release of gas and its impact on permeability of coal. Fuel 69(5):551–556

Heuze FE (1983) High-temperature mechanical, physical and thermal properties of granitic rocks—a review. Int J Rock Mech Min Sci Abstr 20(1):3–10

http.//www.coretest.com/automated-permeameted-porosimeter.html

Kumar H, Elsworth D, Liu J, Pone D, Mathews JP (2015) Permeability evolution of propped artificial fractures in coal on injection of CO_2. J Petrol Sci Eng 133:695–704

Laubach SE, Marrett RA, Olson JE, Scott AR (1998) Characteristics and origins of coal cleat, a review. Int J Coal Geol 35:175–207

Levine JR (1996) Model study of the influence of matrix shrinkage on absolute permeability of coal bed reservoirs. Geol Soc Lond Spec Publ 109(1):197–212

Li S, Dong M, Li Z (2009) Measurement and revised interpretation of gas flow behaviour in tight reservoir cores. J Petroleum Sci Eng 65:81–88

Liu S, Harpalani S (2014) Compressibility of sorptive porous media, Part 2. Experimental study on coal compressibility of sorptive material, experimental study. AAPG Bull 98(9):1773–1788

Liu HH, Rutqvist J (2010) A new coal-permeability model: internal swelling stress and fracture–matrix interaction. Transp Porous Media 82:157–171

Liu J, Wang J, Chen Z, Wang S, Elsworth D, Jiang Y (2011) Impact of transition from local swelling to macro swelling on the evolution of coal permeability. Int J Coal Geol. https://doi.org/10.1016/j.coal.2011.07.008

Liu JF, Skoczylas F, Talandier J (2015) Gas permeability of a compacted bentonite–sand mixture, coupled effects of water content, dry density, and confining pressure. Can Geotechn J 52(8):1159–1167

Liu JF, Song Y, Skoczylas F et al (2016a) Gas migration through water-saturated bentonite–sand mixtures, CO_x argillite and their interfaces. Can Geotech J 53(1):60–71

Liu JF, Skoczylas F, Talandier J, Pu H (2016b) Dismantling of the EB experiment: experimental research on the retrieved GBM and bentonite blocks. Nucl Eng Des 300:297–307

Liu JF, Ni HY, Cao XL et al (2020) Laboratory investigation on gas permeability of compacted GMZ bentonite under a coupled hydraulic-mechanical effect. Eng Geol 276:105761

McKee CR, Bumb AC, Koenig RA (1988) Stress-dependent permeability and porosity of coal and other geologic formations. SPE Form Eval 3(1):81–91

Meng Y, Li Z (2017) Triaxial experiments on adsorption deformation and permeability of different sorbing gases in anthracite coal. J Nat Gas Sci Eng 46:59–70

Meng J, Nie B, Zhao B, Ma Y (2015) Study on law of raw coal seepage during loading process at different gas pressures. Int J Min Sci Technol 25(1):31–35

Palmer I (2009) Permeability changes in coal: analytical modeling. Int J Coal Geol 77(1–2):119–126

Palmer I, Mansoori J (1996) How permeability depends on stress and pore pressure in coalbeds: a new model. SPE Reservoir Eval Eng 1(06):539–544

Palmer I, Mansoori J (1998) How permeability depends on stress and pore pressure in coalbeds: a new model. In: Annual Technical Conference & Exhibition. Society of Petroleum Engineers, Denver, pp 539–544

Palmer I, Mavor M, Gunter B (2007) Permeability changes in coal seams during production and injection. International Coalbed Methane Symposium. University of Alabama, Tuscaloosa, Alabama. Paper 0713.

Pan Z, Connell LD (2011) Modelling of anisotropic coal swelling and its impact on permeability behaviour for primary and enhanced coalbed methane recovery. Int J Coal Geol 85:257–267

Pan Z, Connell LD, Camilleri M (2010) Laboratory characterisation of coal reservoir permeability for primary and enhanced coalbed methane recovery. Int J Coal Geol 2(3–4):252–261

Pei Y, Li SC, Agostini F et al (2019) Sealing of concrete confining structures of French nuclear reactors. Eng Struct 197:109283

Pini R, Ottiger S, Burlini L, Storti G, Mazzotti M (2009) Role of adsorption and swelling on the dynamics of gas injection in coal. J Geophys Res 114(B4)

Robertson EP, Christiansen RL (2005) Measurement of sorption-induced strain. Presented at the 2005 international coalbed methane symposium, Tuscaloosa, Alabama, 17–19 May. Paper 0532.

Seidle, John R., and L. G. Huitt (1995) Experimental measurement of coal matrix shrinkage due to gas desorption and implications for cleat permeability increases. In: International meeting on petroleum Engineering. OnePetro.

Seomoon H, Lee M, Sung W (2015) Analysis of sorption-induced permeability reduction considering gas diffusion phenomenon in coal seam reservoir. Transp Porous Media 108(3):713–729

Shi JQ, Durucan S (2004a) Drawdown induced changes in permeability of coalbeds: a new interpretation of the reservoir response to primary recovery. Transp Porous Media 56:1–16

Shi J-Q, Durucan S (2004b) Drawdown induced changes in permeability of coalbeds: a new interpretation of the reservoir response to primary recovery. Transp Porous Media 56(1):1–16

Shi J-Q, Durucan S (2005) Gas storage and flow in coalbed reservoirs: implementation of a bidisperse pore model for gas diffusion in coal matrix. SPE Reservoir Eval Eng 8(2):169–175

Shi JQ, Durucan S (2010) Exponential growth in San Juan basin Fruitland coalbed permeability with reservoir drawdown: model match and new insights. SPE Reservoir Eval Eng 13(6):914–925

Teng T, Xiaoyan ZHU, Yu-Ming W et al (2021) Experimental investigation of CO_2 seepage behavior in natural fractured coal under hydro-thermal-mechanical conditions. Therm Sci 25(6B):4651–4658

Wang S, Elsworth D, Liu J (2011) Permeability evolution in fractured coal, the roles of fracture geometry and water-content. Int J Coal Geol 87(1):13–25

Wang K, Du F, Wang G (2017) Investigation of gas pressure and temperature effects on the permeability and steady-state time of Chinese anthracite coal, an experimental study. J Nat Gas Sci Eng 40:179–188

Wang L, Chen Z, Wang C, Elsworth D, Liu W (2019) Reassessment of coal permeability evolution using steady-state flow methods: the role of flow regime transition. Int J Coal Geol 211:103210

Wang C, Zhang J, Zang Y, Zhong R, Wang J, Wu Y et al (2021a) Time-dependent coal permeability: Impact of gas transport from coal cleats to matrices. J Nat Gas Sci Eng 88:103806

Wang C, Zhang J, Chen J, Zhong R, Cui G, Jiang Y, Liu W, Chen Z (2021b) Understanding competing effect between sorption swelling and mechanical compression on coal matrix deformation and its permeability. Int J Rock Mech Min Sci 138:104639

Wang C et al (2022) Dynamic analysis of heat extraction rate by supercritical carbon dioxide in fractured rock mass based on a thermal-hydraulic-mechanics coupled model. Int J Min Sci Technol 32(2):225–236

Wong TF, Brace WF (1979) Thermal expansion of rocks, some measurements at high pressure. Tectonophysics 57:95–117

Yanguang X (2019) Research on loose zone of fractured rock roadway based on H-B strength criterion, Chongqing University, China, Master thesis, 2019